Applied Mathematics and Computation 392 (2021) 125677

Contents lists available at ScienceDirect

Applied Mathematics and Computation

journal homepage: www.elsevier.com/locate/amc

Parameter-uniform approximation on equidistributed meshes for singularly perturbed parabolic reaction-diffusion problems with Robin boundary conditions

Sunil Kumar[a,*], Sumit[a], Higinio Ramos[b,c]

[a] Department of Mathematical Sciences, Indian Institute of Technology (BHU) Varanasi, 221005, Uttar Pradesh, India
[b] Scientific Computing Group, Universidad de Salamanca, Plaza de la Merced, Salamanca 37008, Spain
[c] Escuela Politcnica Superior de Zamora, Campus Viriato, Zamora 49022, Spain

ARTICLE INFO

Article history:
Received 8 April 2020
Revised 28 July 2020
Accepted 13 September 2020

Keywords:
Boundary layers
Robin boundary conditions
Adaptive mesh
Equidistribution principle

ABSTRACT

In this work we develop a parameter-uniform numerical method on equidistributed meshes for solving a class of singularly perturbed parabolic reaction-diffusion problems with Robin boundary conditions. The discretization consists of a modified Euler scheme in time, a central difference scheme in space, and a special finite difference scheme for the Robin boundary conditions. A uniform mesh is used in the time direction while the mesh in the space direction is generated via the equidistribution of a suitably chosen monitor function. We discuss error analysis and prove that the method is parameter-uniformly convergent of order two in space and order one in time. To support the theoretical result, some numerical experiments are performed.

© 2020 Elsevier Inc. All rights reserved.

1. Introduction

Singularly perturbed problems are among the ones having solutions with multi-scale character, for which one part of the solution varies smoothly and the other part varies rapidly. These often arise in various fields of applied mathematics and engineering, such as fluid dynamics, optimal control theory, elasticity, population dynamics, oceanography, quantum mechanics, and so on. This interesting behavior of the solutions and the regular occurrence of these problems make scientists and mathematicians eager to work for their solutions [1–6]. In this paper, we consider the following singularly perturbed time-dependent problem

$$\begin{cases} \mathcal{L}y := \frac{\partial y}{\partial t} + \mathcal{L}_\varepsilon y = f(x,t), \quad (x,t) \in (0,1) \times (0,T], \\ \mathcal{D}_l y(0,t) := y(0,t) - \sqrt{\varepsilon}\frac{\partial y}{\partial x}(0,t) = \phi_l(t), \ \ t \in (0,T], \\ \mathcal{D}_r y(1,t) := y(1,t) + \sqrt{\varepsilon}\frac{\partial y}{\partial x}(1,t) = \phi_r(t), \ \ t \in (0,T], \\ y(x,0) = \phi_b(x), \ \ x \in [0,1], \end{cases} \tag{1.1}$$

where $\mathcal{L}_\varepsilon y := -\varepsilon \frac{\partial^2 y}{\partial x^2} + a(x)y$ and $0 < \varepsilon \leq 1$ is a small positive constant called the perturbation parameter. The functions $a(x)$ and $f(x, t)$ are assumed to be sufficiently smooth on their respective domains, with $0 < \alpha \leq a(x)$ on [0,1]. It is known

* Corresponding author.
E-mail addresses: skumar.iitd@gmail.com (S. Kumar), sumit.rs.mat16@itbhu.ac.in (Sumit), higra@usal.es (H. Ramos).

https://doi.org/10.1016/j.amc.2020.125677
0096-3003/© 2020 Elsevier Inc. All rights reserved.

that the solution exhibits layers near the boundaries $x = 0$ and $x = 1$, and further the solution $y(x, t)$ can be decomposed as a sum of a regular part v and a singular part w, satisfying [7,8]

$$\left\| \frac{\partial^{p+q} y}{\partial x^p \partial t^q} \right\| < C\varepsilon^{-\frac{p}{2}}, \quad \text{for } 1 \le p + 2q \le 4, \ \ p, q \in \mathbb{N}_0, \tag{1.2}$$

$$\left\| \frac{\partial^{p+q} v}{\partial x^p \partial t^q} \right\| < C \quad \text{and} \quad \left| \frac{\partial^{p+q} w}{\partial x^p \partial t^q} \right| < C\varepsilon^{-\frac{p}{2}} (e^{-x\sqrt{\frac{\alpha}{\varepsilon}}} + e^{-(1-x)\sqrt{\frac{\alpha}{\varepsilon}}}), \quad \text{for } 1 \le p + 2q \le 4, \ \ p, q \in \mathbb{N}_0. \tag{1.3}$$

Inside the layer regions the solution varies very rapidly and this would demand a uniform mesh with mesh size $\mathcal{O}(1/\varepsilon)$ for standard methods to resolve the layers, which is computationally very costly and not feasible. Therefore, we require special meshes that are able to resolve the layers yielding a parameter-uniform accuracy, meaning that the approximate solution should converge to the exact solution independently of the perturbation parameter [1,3,9].

Special fitted meshes like Shishkin [10] and Bakhvalov [11] meshes are few good and favourable options for standard methods to produce satisfactory results. But the success of these meshes relies on good a priori knowledge of the location and size of the layer(s). Otherwise, we need an algorithm which can itself detect the location and width of the layer(s) and can construct an adaptive mesh. One of the most popular adaptive mesh algorithms is based on the equidistribution principle [12]. Starting with a uniform mesh, this technique aims to condense the maximum number of mesh points inside the layer region(s). At any time level t_k, the mesh $\{x_i^k\}_{i=0}^N$ is said to be equidistributed with respect to the monitor function $\mathcal{M}(y(x,t_k),x)$ if

$$\int_{x_{i-1}^k}^{x_i^k} \mathcal{M}(y(z,t_k),z)dz = \frac{1}{N}\int_0^1 \mathcal{M}(y(z,t_k),z)dz, \quad 1 \le i \le N. \tag{1.4}$$

Although this idea has been applied to many practical problems, very little progress has been made on its analysis. Based on the problem considered and the expected order of convergence of the numerical schemes, few different monitor functions have been suggested in Das and Natesan [13], Qiu and Sloan [14], Mackenzie [15], Gowrisankar and Natesan [16], Beckett and Mackenzie [17], Kopteva et al. [18], Das et al. [19], Liu et al. [20], Das and Mehrmann [21], Das [22,23].

Singularly perturbed problems similar to (1.1) with Dirichlet type boundary conditions have been studied extensively in the literature (see [24–31] and the references therein). However, there are only few studies of such problems with Robin boundary conditions (RBCs) [7,8,32,33]. Note that all of these studies considered Shishkin meshes to resolve the layers and to develop parameter-uniform numerical methods. As per our knowledge, in the literature there is no result considering the approximation of a time-dependent problem with Robin's boundary conditions on layer-adaptive equidistributed meshes. So, in this paper, we aim to construct a parameter-uniform numerical method on equidistributed meshes for problem (1.1). We generate the adaptive mesh at each time level based on a suitable monitor function $\mathcal{M}$. The time derivative is discretized by a modified Euler's scheme, the space derivative is discretized by the central difference scheme, and the Robin's boundary conditions are approximated by a special finite difference scheme to maintain the accuracy. We provide the convergence analysis of the proposed method and prove that the method is parameter-uniform accurate of first order in time and second order in space. Some numerical experiments are conducted in order to validate our theoretical results and effectiveness of the method.

This paper is structured as follows: The problem discretization and the adaptive mesh formation are given in Section 2. In Section 3, the error analysis of the proposed method is studied. Section 4 is devoted to the results and discussion of numerical experiments on two test examples. Then the paper concludes with Section 5. The appendix is devoted to the error analysis for a stationary version of problem (1.1).

Notation: We use C for any generic positive constant, which is independent of ε, M and N. We denote the maximum norm $\max_{(x,t)\in[0,1]\times[0,T]} |g(x,t)|$ by $\|g\|$ for any function g defined on the domain $[0, 1] \times [0, T]$. $\mathbb{N}_0 = \{0, 1, 2, \dots\}$.

2. Discretization and adaptive mesh generation

2.1. The discretization strategy

In time direction we take a uniform mesh $\{t_j\}_{j=0}^M$ with step size $\Delta t = T/M$, where M is the number of mesh intervals. Then an arbitrary non-uniform spatial mesh is considered at any time level t_j denoted by $\{x_i^j\}_{i=0}^N$ with step sizes $h_i^j = x_i^j - x_{i-1}^j, i = 1, \dots, N$. Thus, the complete discretization of the domain is the tensor product of these two one-dimensional meshes. On this discrete domain, problem (1.1) is discretized by

$$\begin{cases} \left[L^{N,M}Y\right]_i^j := \delta_t^\star Y_i^j + \left[L_\varepsilon^{N,M}Y\right]_i^j = f_i^j, \quad i = 1,\dots,N-1, \ \ j = 1,\dots,M, \\ \left[D_l^{N,M}Y\right]_0^j := Y_0^j - \sqrt{\varepsilon}D_x^+Y_0^j + \frac{h_1^j}{2\sqrt{\varepsilon}}\left(a_0Y_0^j + \delta_t^\star Y_0^j\right) = \phi_l^j + \frac{h_1^j}{2\sqrt{\varepsilon}}f_0^j, \quad j = 1,\dots,M, \\ \left[D_r^{N,M}Y\right]_N^j := Y_N^j + \sqrt{\varepsilon}D_x^-Y_N^j + \frac{h_N^j}{2\sqrt{\varepsilon}}\left(a_NY_N^j + \delta_t^\star Y_N^j\right) = \phi_r^j + \frac{h_N^j}{2\sqrt{\varepsilon}}f_N^j, \quad j = 1,\dots,M, \\ Y_i^0 = \phi_{b;i}, \quad i = 0,\dots,N, \end{cases} \tag{2.1}$$

where

$$[L_\varepsilon^{N,M}Y]_i^j := -\varepsilon\delta_x^2 Y_i^j + a_i Y_i^j, \quad \delta_t^\star Y_i^j = \frac{Y_i^j - \widetilde{Y}_i^{j-1}}{\Delta t},$$

$$D_x^+ Y_i^j = \frac{Y_{i+1}^j - Y_i^j}{h_{i+1}^j}, \quad D_x^- Y_i^j = \frac{Y_i^j - Y_{i-1}^j}{h_i^j}, \quad \delta_x^2 Y_i^j = \frac{(D_x^+ - D_x^-)Y_i^j}{(h_i^j + h_{i+1}^j)/2},$$

$a_i = a(x_i^j)$, $f_i^j = f(x_i^j, t_j)$, $\phi_{b;i} = \phi_b(x_i^j)$, and $\widetilde{Y}_i^{j-1} = Y(x_i^j, t_{j-1})$ is obtained by evaluating the piecewise linear interpolation of $Y_i^{j-1} = Y(x_i^{j-1}, t_{j-1}), 0 \le i \le N$, at the point x_i^j. We also define $[D_{r,x}^{N,M}Y]_N^j := Y_N^j + \sqrt{\varepsilon}D_x^- Y_N^j + \frac{h_N^j}{2\sqrt{\varepsilon}}a_N Y_N^j$ and $[D_{l,x}^{N,M}Y]_0^j := Y_0^j - \sqrt{\varepsilon}D_x^+ Y_0^j + \frac{h_1^j}{2\sqrt{\varepsilon}}a_0 Y_0^j$, that we shall use later in Section 3. Using standard arguments we can prove that the following discrete maximum principle holds [8].

Lemma 1. *(Discrete maximum principle) Consider a mesh function U such that $[L^{N,M}U]_i^j \ge 0$ for $i = 1, \dots, N-1$, $j = 1, \dots, M$, and $[D_l^{N,M}U]_0^j \ge 0$, $[D_r^{N,M}U]_N^j \ge 0$ for $j = 1, \dots, M$. Then $U_i^j \ge 0$ for $i = 0, \dots, N$, $j = 0, \dots, M$.*

2.2. Adaptive mesh

The solution of the problem (1.1) possesses boundary layers, so we need a layer resolving mesh in the spatial direction. We here construct the layer resolving mesh using the equidistribution principle. The following monitor function is considered

$$\mathcal{M}(y(x,t_k),x) = \aleph^k + \left|\frac{\partial^2 w}{\partial x^2}(x,t_k)\right|^{1/2}, \tag{2.2}$$

where $\aleph^k$ is chosen according to the specifications in Lemma 2, below. A similar monitor function is also considered in Gowrisankar and Natesan [16], Beckett and Mackenzie [17] for problems with Dirichlet boundary conditions. Using this monitor function, the equidistributed mesh at any time t_k can be obtained by using the following relation

$$\int_0^{x^k(\xi)} \mathcal{M}(y(z,t_k),z)dz = \xi \int_0^1 \mathcal{M}(y(z,t_k),z)dz, \quad \xi \in [0,1], \tag{2.3}$$

which is equivalent to (1.4). To get the structure of the mesh generated using (2.3), we follow the similar approach as in Beckett and Mackenzie [17], Das and Vigo-Aguiar [34]. Consider the derivative bounds of w from (1.3) to approximate $\frac{\partial^2 w}{\partial x^2}$ as

$$\frac{\partial^2 w}{\partial x^2}(x,t_k) \approx \begin{cases} \frac{\nu_1}{\varepsilon}e^{-x\sqrt{\frac{\alpha}{\varepsilon}}}, & x \in [0,1/2], \\ \frac{\nu_2}{\varepsilon}e^{-(1-x)\sqrt{\frac{\alpha}{\varepsilon}}}, & x \in [1/2,1], \end{cases}$$

where ν_1 and ν_2 are constants, independent of ε and x. So,

$$\int_0^1 \left|\frac{\partial^2 w}{\partial x^2}(z,t_k)\right|^{1/2} dz \equiv \mathbf{A} \approx 2\left[\frac{|\nu_1|^{1/2} + |\nu_2|^{1/2}}{\alpha^{1/2}}\right].$$

Hence, from (2.2) and (2.3), for $x^k(\xi) \le \frac{1}{2}$, we have the mapping

$$\xi\left(\frac{\aleph^k}{\mathbf{A}} + 1\right) = \frac{\aleph^k}{\mathbf{A}}x^k(\xi) + \lambda_1\left(1 - e^{-\frac{x^k(\xi)}{2}\sqrt{\frac{\alpha}{\varepsilon}}}\right), \tag{2.4}$$

where

$$\lambda_1 = \frac{|\nu_1|^{1/2}}{|\nu_1|^{1/2} + |\nu_2|^{1/2}}.$$

Similarly, for $x^k(\xi) > \frac{1}{2}$, the equidistribution principle gives

$$(1-\xi)\left(\frac{\aleph^k}{\mathbf{A}} + 1\right) = \frac{\aleph^k}{\mathbf{A}}(1 - x^k(\xi)) + \lambda_2\left(1 - e^{-\frac{1-x^k(\xi)}{2}\sqrt{\frac{\alpha}{\varepsilon}}}\right), \tag{2.5}$$

where

$$\lambda_2 = \frac{|\nu_2|^{1/2}}{|\nu_1|^{1/2} + |\nu_2|^{1/2}}.$$

Thus, corresponding to a uniform mesh $\{\xi_i^k = i/N\}_{i=0}^N$ in computational space we obtain a non-uniform mesh $\{x_i^k\}_{i=0}^N$ in physical space at each time level using the following relations

$$\frac{i}{N}(\frac{\aleph^k}{\mathbf{A}}+1) = \frac{\aleph^k}{\mathbf{A}}x_i^k + \lambda_1(1-e^{-\frac{x_i^k}{2}\sqrt{\frac{\alpha}{\varepsilon}}}), \quad x_i^k \le 1/2 \tag{2.6}$$

and

$$(1-\frac{i}{N})(\frac{\aleph^k}{\mathbf{A}}+1) = \frac{\aleph^k}{\mathbf{A}}(1-x_i^k) + \lambda_2(1-e^{-\frac{(1-x_i^k)}{2}\sqrt{\frac{\alpha}{\varepsilon}}}), \quad x_i^k > 1/2. \tag{2.7}$$

The following lemma provides information about the distribution of the mesh points and also gets some bounds on the mesh spacing.

Lemma 2. *Taking $\aleph^k = \mathbf{A}$, the nonuniform mesh generated by (2.6) and (2.7) satisfies*

$$x_\ell^k < 2\sqrt{\frac{\varepsilon}{\alpha}}\log N < x_{\ell+1}^k \quad \text{and} \quad x_{r-1}^k < 1-2\sqrt{\frac{\varepsilon}{\alpha}}\log N < x_r^k, \tag{2.8}$$

where

$$\ell = \left[\frac{1}{2}\left(2\sqrt{\frac{\varepsilon}{\alpha}}N\log N + \lambda_1(N-1)\right)\right], r = \left[N - \frac{1}{2}\left(2\sqrt{\frac{\varepsilon}{\alpha}}N\log N + \lambda_2(N-1)\right)\right]+1$$

and $[\ \cdot\ ]$ is the integer part function. Moreover, the mesh spacing satisfies

$$h_i^k < C\sqrt{\frac{\varepsilon}{\alpha}} \quad \text{for } i = 1,\dots,\ell \text{ and } i = r+1,\dots,N-1 \tag{2.9}$$

with

$$|h_{i+1}^k - h_i^k| \le C(h_i^k)^2 \quad \text{for } i = 1,\dots,\ell-1 \quad \text{and} \quad |h_{i+1}^k - h_i^k| \le C(h_{i+1}^k)^2 \quad \text{for } i = r+1,\dots,N-1. \tag{2.10}$$

Further, we have

$$h_i^k \le CN^{-1} \quad \text{for } i = 1,\dots,N. \tag{2.11}$$

Proof. The proof of (2.8)–(2.10) can be obtained using arguments similar to those in Beckett and Mackenzie [17]. To prove (2.11), we use the idea in Das and Natesan [13], Das et al. [19]. Note that for the monitor function (2.2) we have $\mathbf{A} = \aleph^k \le \mathcal{M}(y(x,t_k),x)$. So, using the derivative bounds we get

$$\int_0^1 \mathcal{M}(y(z,t_k),z)dz \le C.$$

Thus, by the equidistribution principle, we get

$$\aleph^k h_i^k \le \int_{x_{i-1}^k}^{x_i^k} \mathcal{M}(y(z,t_k),z)dz = \frac{1}{N}\int_0^1 \mathcal{M}(y(z,t_k),z)dz \le CN^{-1}.$$

Hence, $h_i^k \le CN^{-1}$. □

3. Error analysis

The parameter-uniform convergence analysis of the difference scheme (2.1) is provided in the following theorem.

Theorem 3.1. *Let $y(x_i^j,t_j)$ and Y_i^j be the solutions of (1.1) and (2.1), respectively. If for some $0 < \gamma < 1$ it is $N^{-\gamma} \le C\Delta t$, then for $i = 0,\dots,N,\ j = 0,\dots,M$, we have the following bound*

$$|y(x_i^j,t_j) - Y_i^j| \le C(\Delta t + N^{-2+\gamma}).$$

Proof. Suppose $\eta_i^j = y(x_i^j,t_j) - Y_i^j$ denotes the error in the numerical solution at (x_i^j,t_j). So, we can write the truncation error as follows

$$[\delta_t^\star \eta]_i^j + [L_\varepsilon^{N,M}\eta]_i^j = \mathcal{X}_{1;i}^j + \mathcal{X}_{2;i}^j \text{ for } i = 1,\dots,N-1,\ \ j = 1,\dots,M,$$

where

$$\mathcal{X}_{1;i}^j = [L_\varepsilon^{N,M}y]_i^j - (\mathcal{L}_\varepsilon y)_i^j \quad \text{and} \quad \mathcal{X}_{2;i}^j = \delta_t^\star y(x_i^j,t_j) - \frac{\partial y}{\partial t}(x_i^j,t_j).$$

Also,

$$[D_l^{N,M}\eta]_0^j = \zeta_{l,1;0}^j + \zeta_{l,2;0}^j,$$

$$[D_r^{N,M}\eta]_N^j = \zeta_{r,1;N}^j + \zeta_{r,2;N}^j,$$

where

$$\zeta_{l,1;0}^j = [D_{l,x}^{N,M}y]_0^j - \left((D_l y)_0^j + \frac{h_1^j}{2\sqrt{\varepsilon}}(\mathcal{L}_\varepsilon y)_0^j\right), \quad \zeta_{l,2;0}^j = \frac{h_1^j}{2\sqrt{\varepsilon}}(\delta_t^\star y(x_0^j,t_j) - \frac{\partial y}{\partial t}(x_0^j,t_j)),$$

$$\zeta_{r,1;N}^j = [D_{r,x}^{N,M}y]_N^j - \left((D_r y)_N^j + \frac{h_N^j}{2\sqrt{\varepsilon}}(\mathcal{L}_\varepsilon y)_N^j\right), \quad \text{and} \quad \zeta_{r,2;N}^j = \frac{h_N^j}{2\sqrt{\varepsilon}}(\delta_t^\star y(x_N^j,t_j) - \frac{\partial y}{\partial t}(x_N^j,t_j)).$$

Now we split the error η_i^j as $\eta_i^j = \rho_i^j + \omega_i^j$, where ρ_i^j, for each fixed j, is the solution of the following stationary discrete problem

$$\begin{cases} \left[L_\varepsilon^{N,M}\rho\right]_i^j = \mathcal{X}_{1;i}^j, \ i = 1,\dots,N-1, \\ \left[D_{l,x}^{N,M}\rho\right]_0^j = \zeta_{l,1;0}^j, \\ \left[D_{r,x}^{N,M}\rho\right]_N^j = \zeta_{r,1;N}^j, \end{cases} \tag{3.1}$$

and ω_i^j is the solution of the following parabolic discrete problem

$$\begin{cases} \left[\delta_t^\star\omega + L_\varepsilon^{N,M}\omega\right]_i^j = \mathcal{X}_{2;i}^j - \delta_t^\star\rho_i^j, \ i = 1,\dots,N-1, \ j = 1,\dots,M, \\ \left[D_l^{N,M}\omega\right]_0^j = \zeta_{l,2;0}^j - \frac{h_1^j}{2\sqrt{\varepsilon}}\delta_t^\star\rho_0^j, \ j = 1,\dots,M, \\ \left[D_r^{N,M}\omega\right]_N^j = \zeta_{r,2;N}^j - \frac{h_N^j}{2\sqrt{\varepsilon}}\delta_t^\star\rho_N^j, \ j = 1,\dots,M, \\ \omega_i^0 = -\rho_i^0, \ i = 0,\dots,N. \end{cases} \tag{3.2}$$

Here we see that equation (3.1) is the same that we obtain when we analyse the error component ρ in a stationary problem that is discretized using $\mathcal{L}_\varepsilon$ with Robin boundary conditions, and $\mathcal{X}_{1,i}^j, \zeta_{l,1;0}^j, \zeta_{r,1;N}^j$, the corresponding truncation errors (see Appendix A.1). So, we can invoke the error bound of Appendix A.1 to get

$$|\rho_i^j| \le CN^{-2} \quad \text{for all } i, j. \tag{3.3}$$

Now we shall obtain a bound for the error component ω_i^j. Note that the problem (3.2) is similar to the discrete problem (2.1). Hence, using the discrete maximum principle (Lemma 1) we get

$$|\omega_i^j| \le C(\max_i|\rho_i^0| + \max_j|[D_l^{N,M}\omega]_0^j| + \max_j|[D_r^{N,M}\omega]_N^j| + \max_{i,j}|\mathcal{X}_{2;i}^j - \delta_t^\star\rho_i^j|) \le C(\Delta t + N^{-2+\gamma} + \max_{i,j}|\delta_t^\star\rho_i^j|), \tag{3.4}$$

where we have used the triangle inequality, the inequality in (3.3), and the fact that $\mathcal{X}_{2,i}^j, \zeta_{l,2;0}^j$, and $\zeta_{r,2;N}^j$ are bounded by $C(\Delta t + N^{-2+\gamma})$ for some $0 < \gamma < 1$ such that $N^{-\gamma} \le C\Delta t$, which can be verified using Taylor expansion, standard interpolation error estimates, and (1.2). So, now it remains to bound the term $\delta_t^\star\rho_i^j$ in (3.4). Using (3.1), a straightforward calculation shows that $\delta_t^\star\rho_i^j$ satisfies

$$\begin{cases} \left[L_\varepsilon^{N,M}\delta_t^\star\rho\right]_i^j = \delta_t^\star\mathcal{X}_{1;i}^j, \ i = 1,\dots,N-1, \\ \left[D_{l,x}^{N,M}\delta_t^\star\rho\right]_0^j = \delta_t^\star\zeta_{l,1;0}^j, \\ \left[D_{r,x}^{N,M}\delta_t^\star\rho\right]_N^j = \delta_t^\star\zeta_{r,1;N}^j. \end{cases} \tag{3.5}$$

To analyse the problem (3.5), we write the right hand side as

$$\begin{aligned} \delta_t^\star\mathcal{X}_{1;i}^j &= \frac{1}{\Delta t}\left[\mathcal{X}_{1;i}^j - \widetilde{\mathcal{X}}_{1;i}^{j-1}\right] \\ &= \frac{1}{\Delta t}\Big[\left([L_\varepsilon^{N,M}y]_i^j - (\mathcal{L}_\varepsilon y)_i^j\right) - \Big(\left([L_\varepsilon^{N,M}y]_{n-1}^{j-1} - (\mathcal{L}_\varepsilon y)_{n-1}^{j-1}\right)\psi_{n-1}(x_i^j) \\ &\quad + \left([L_\varepsilon^{N,M}y]_n^{j-1} - (\mathcal{L}_\varepsilon y)_n^{j-1}\right)\psi_n(x_i^j)\Big)\Big], \end{aligned}$$

where

$$\psi_{n-1}(x) = \frac{x_n^{j-1} - x}{x_n^{j-1} - x_n^{j-1}} \text{ and } \psi_n(x) = \frac{x - x_{n-1}^{j-1}}{x_n^{j-1} - x_{n-1}^{j-1}} \text{ with } x_{n-1}^{j-1} \le x_i^j \le x_{n-1}^j \text{ for some } n.$$

Set $\check{\mathcal{L}}_\varepsilon y = -\varepsilon \frac{\partial^2 y}{\partial x^2}$ and suppose its discretization is $[\check{L}_\varepsilon^{N,M} Y]_i^j = -\varepsilon \delta_x^2 Y_i^j$. Now by using the fact that the linear interpolation error is $\mathcal{O}(N^{-2})$, we can write

$$|\delta_t^\star \mathcal{X}_{1,i}^j| \le \left| \frac{1}{\Delta t} \int_{t_{j-1}}^{t_j} \left[\check{L}_\varepsilon^{N,M} \frac{\partial y}{\partial t}(x_i^j, t) - \check{\mathcal{L}}_\varepsilon \frac{\partial y}{\partial t}(x_i^j, t) \right] dt \right| + CN^{-2+\gamma}.$$

Thus, using the Peano kernel theorem [35,36] and the bounds in (1.2), we get the same bound for $\delta_t^\star \mathcal{X}_{1;i}^j$ that we get for the corresponding truncation error for stationary problem. Similarly we can obtain also same bounds for $\delta_t^\star \zeta_{l,1;0}^j$ and $\delta_t^\star \zeta_{r,1;N}^j$. Hence, we get $\delta_t^\star \rho_i^j \le CN^{-2+\gamma}$ for all *i, j*. Therefore, on combining (3.3) and (3.4) we get the desired result. □

Remark 3.1. The assumption $N^{-\gamma} \le C\Delta t$ for some $0 < \gamma < 1$ used in the above theorem is for the theoretical proof only. However, in the numerical experiments there is no influence of this restriction on the parameter-uniform convergence behavior. Such an assumption is common in the literature (see, e.g. [21]).

4. Numerical experiments

We now present the numerical experiments that we performed for two test examples to verify our theoretical result. To construct the adaptive mesh we use Algorithm 1. In the stopping criterion we have taken the value $\varrho = 1.1$. As the second

---

Algorithm 1: Algorithm for the adaptive mesh and adaptive solution.

Input: $N, M \in \mathbb{N}, 0 < \varepsilon \le 1$ and $\varrho > 1$.
Output: Adaptive mesh $\{x_i^k\}$ and adaptive solution Y_i^k at each time level t_k.

Step **Initialization:** Initialize the mesh (for iteration $r = 1$) taking $\{x_i^{k,(r)}\}$ as the uniform mesh for $k = 1$, otherwise x^{k-1} for kth time level.

Step Solve the discrete problem (2.1) for $Y_i^{k,(r)}$ on $\{x_i^{k,(r)}\}$.

Step Find the discrete monitor function defined by

$$\mathcal{M}_i^{k,(r)} = \aleph^{k,(r)} + |\delta_x^2 Y_i^{k,(r)}|^{1/2}, \text{ for } i = 1, \dots, N-1,$$

where $\aleph^{k,(r)}$ is defined by

$$\aleph^{k,(r)} = h_1^{k,(r)} |\delta_x^2 Y_1^{k,(r)}|^{1/2} + \sum_{i=2}^{N-1} h_i^{k,(r)} \left\{ \frac{|\delta_x^2 Y_{i-1}^{k,(r)}|^{1/2} + |\delta_x^2 Y_i^{k,(r)}|^{1/2}}{2} \right\} + h_N^{k,(r)} |\delta_x^2 Y_{N-1}^{k,(r)}|^{1/2}.$$

Step Set $H_i^{k,(r)} = h_i^{k,(r)} \left(\frac{\mathcal{M}_{i-1}^{k,(r)} + \mathcal{M}_i^{k,(r)}}{2} \right)$ for $i = 1, \dots, N$, take $\mathcal{M}_0^{k,(r)} = \mathcal{M}_1^{k,(r)}$ and $\mathcal{M}_N^{k,(r)} = \mathcal{M}_{N-1}^{k,(r)}$. Then define $L_i^{k,(r)}$ by $L_i^{k,(r)} = \sum_{j=1}^{i} H_j^{k,(r)}$ for $i = 1, \dots, N$ and $L_0^{k,(r)} = 0$.

Step **Stopping criterion**: Define $\varrho^{(r)}$ by $\varrho^{(r)} = \frac{N}{L_N^{k,(r)}} \max_{i=1,\dots,N} H_i^{k,(r)}$. Go to Step 7 if $\varrho^{(r)} \le \varrho$, else continue with Step 6.

Step Define $Z_i^{k,(r)} = i \frac{L_N^{k,(r)}}{N}$ for $i = 0, 1, \dots, N$. New mesh $\{x_i^{k,(r+1)}\}$ is generated by evaluating the interpolant function of the points $(L_i^{k,(r)}, x_i^{k,(r)})$ at $Z_i^{k,(r)}$, set $r = r + 1$ and return to Step 2.

Step Take $\{x_i^{k,(r-1)}\}$ as the final layer adaptive mesh and $Y_i^{k,(r-1)}$ as the required adaptive solution at the k-th time level.

Step Go to Step 1 with $k = k + 1$, repeat the same process for the adaptive mesh and solution at $(k+1)$th time level.

---

derivative of the smooth part v is bounded independently of ε, in practice, it is observed that the monitor function with w replaced by y also produces similar layer-adapted meshes and numerical results [19].

Example 4.1. Consider the problem

$$\begin{cases} \frac{\partial y}{\partial t} - \varepsilon \frac{\partial^2 y}{\partial x^2} + \frac{1+x^2}{2} y = t^3, \quad (x,t) \in (0,1) \times (0,1], \\ \mathcal{D}_l y(0,t) = -\frac{128}{35} \pi^{-1/2} t^{7/2}, \ t \in (0,1], \\ \mathcal{D}_r y(1,t) = -\frac{128}{35} \pi^{-1/2} t^{7/2}, \ t \in (0,1], \\ y(x,0) = 0, \ x \in [0,1]. \end{cases}$$

The surface plot in Fig. 1 displays the numerical solution of Example 4.1 for $\varepsilon = 10^{-4}$ with $N = 128$ and $M = 32$. This clearly shows the existence of boundary layers near $x = 0$ and $x = 1$. The exact solution of Example 4.1 is unknown, so the maximum pointwise errors and rates of convergence are calculated by using the double mesh principle. We bisect the meshes in space and time, and calculate the pointwise errors at the coarse mesh points using the formula

$$G_{i,k}^{\varepsilon,N,M} = |Y_{2i}^{2k,2N,2M} - Y_i^{k,N,M}|.$$

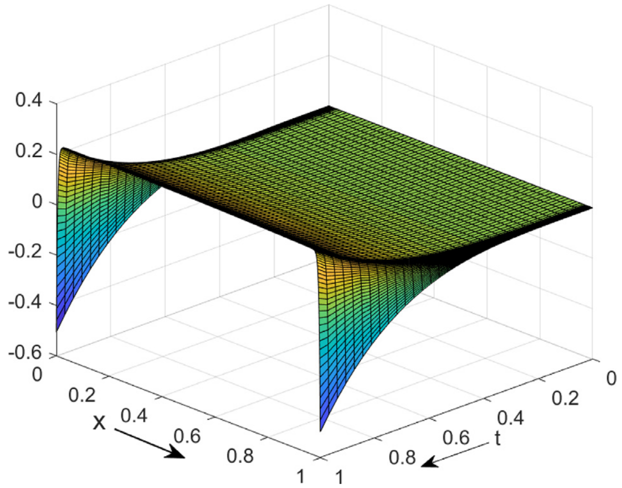

Fig. 1. Surface plot of the numerical solution of Example 4.1 with $N = 128$, $M = 32$, and $\varepsilon = 10^{-4}$.

Table 1
Errors and convergence rates for Example 4.1.

ε	$N = 32$ $M = 8$	$N = 64$ $M = 16$	$N = 128$ $M = 32$	$N = 256$ $M = 64$	$N = 512$ $M = 128$
10^{0}	3.2130e−02	1.6470e−02	8.3343e−03	4.1915e−03	2.1018e−03
	0.9641	0.9827	0.9916	0.9958	
10^{-1}	9.5181e−03	5.0272e−03	2.5857e−03	2.1018e−03	6.5953e−04
	0.9209	0.9592	2.9895	1.6721	
10^{-2}	2.4266e−02	1.1996e−02	5.9569e−03	2.9678e−03	1.4812e−03
	1.0164	1.0099	1.0052	1.0027	
10^{-3}	2.5267e−02	1.2420e−02	6.1519e−03	3.0609e−03	1.5266e−03
	1.0246	1.0135	1.0071	1.0036	
10^{-4}	2.5445e−02	1.2489e−02	6.1824e−03	3.0754e−03	1.5336e−03
	1.0268	1.0144	1.0074	1.0038	
10^{-5}	2.5488e−02	1.2505e−02	6.1883e−03	3.0776e−03	1.5346e−03
	1.0274	1.0149	1.0077	1.0039	
10^{-6}	2.5493e−02	1.2507e−02	6.1893e−03	3.0780e−03	1.5348e−03
	1.0274	1.0149	1.0078	1.0039	
10^{-7}	2.5495e−02	1.2507e−02	6.1897e−03	3.0782e−03	1.5348e−03
	1.0275	1.0148	1.0078	1.0040	
10^{-8}	2.5497e−02	1.2508e−02	6.1896e−03	3.0782e−03	1.5348e−03
	1.0275	1.0149	1.0078	1.0040	
$G^{N,M}$	3.2130e−02	1.6470e−02	8.3343e−03	4.1915e−03	2.1018e−03
$F^{N,M}$	0.9641	0.9827	0.9916	0.9958	

Using these values, the maximum pointwise errors and the parameter-uniform errors are calculated by

$$G^{\varepsilon,N,M} = \max_{i,k} G_{i,k}^{\varepsilon,N,M} \quad \text{and} \quad G^{N,M} = \max_{\varepsilon} G^{\varepsilon,N,M},$$

respectively. We then calculate the rates of convergence and the parameter-uniform rates of convergence by

$$F^{\varepsilon,N,M} = \log_2\left(\frac{G^{\varepsilon,N,M}}{G^{\varepsilon,2N,2M}}\right) \quad \text{and} \quad F^{N,M} = \log_2\left(\frac{G^{N,M}}{G^{2N,2M}}\right),$$

respectively. The numerical results for Example 4.1 are presented in Table 1. From this table, we observe that the error is decreasing as the number of mesh points is increasing. Moreover, the rate of convergence is one. This is due to the fact that the time discretization errors are dominating the global errors in this case. In order to show the contribution of the space discretization errors to the global errors we calculate the following convergence rates

$$\widehat{F}^{\varepsilon,N,M} = \log_2\left(\frac{G^{\varepsilon,N,M}}{G^{\varepsilon,2N,4M}}\right) \quad \text{and} \quad \widehat{F}^{N,M} = \log_2\left(\frac{G^{N,M}}{G^{2N,4M}}\right).$$

Observe that the number of mesh points in space is doubled, whereas the number of mesh points in time is quadrupled. In this way, the contributions of time and space discretizations are balanced. The results are displayed in Table 2. From these results, we observe that the rate of convergence is two.

Table 2
Errors and convergence rates for Example 4.1.

ε	$N=32$ $M=8$	$N=64$ $M=32$	$N=128$ $M=128$	$N=256$ $M=512$	$N=512$ $M=2048$
10^{0}	3.2130e−02	8.3210e−03	2.980e−03	5.2559e−04	1.3143e−04
	1.9490	1.9877	1.9969	1.9995	
10^{-1}	9.5181e−03	2.5657e−03	6.5031e−04	1.6078e−04	4.0673e−05
	1.8193	1.9801	2.0160	1.9829	
10^{-2}	2.4266e−02	5.9485e−03	1.4783e−03	3.6896e−04	9.2221e−05
	2.0283	2.0084	2.0024	2.0003	
10^{-3}	2.5267e−02	6.1456e−03	1.5248e−03	3.8039e−04	9.5049e−05
	2.0396	2.0108	2.0031	2.0007	
10^{-4}	2.5445e−02	6.1794e−03	1.5329e−03	3.8240e−04	9.5546e−05
	2.0418	2.0112	2.0030	2.0008	
10^{-5}	2.5488e−02	6.1871e−03	1.5342e−03	3.8272e−04	9.5608e−05
	2.0425	2.0117	2.0032	2.0011	
10^{-6}	2.5493e−02	6.1889e−03	1.5345e−03	3.8278e−04	9.5627e−05
	2.0423	2.0119	2.0032	2.0011	
$G^{N,M}$	3.2130e−02	8.3210e−03	2.980e−03	5.2559e−04	1.3143e−04
$\widehat{F}^{N,M}$	1.9490	1.9877	1.9969	1.9995	

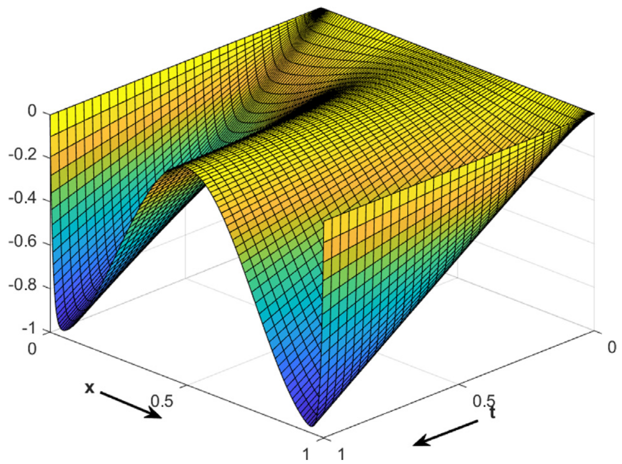

Fig. 2. Surface plot of the numerical solution of Example 4.2 with $N=128$, $M=32$, and $\varepsilon=10^{-4}$.

Example 4.2. Consider the problem

$$\begin{cases} \frac{\partial y}{\partial t} - \varepsilon \frac{\partial^2 y}{\partial x^2} + \left(1 + xe^{-t}\right)y = f(x,t), \quad (x,t) \in (0,1) \times (0,1], \\ \mathcal{D}_l y(0,t) = \phi_l(t), \ t \in (0,1], \\ \mathcal{D}_r y(1,t) = \phi_r(t), \ t \in (0,1], \\ y(x,0) = 0, \ x \in [0,1], \end{cases}$$

where the functions $f(x, t), \phi_l(t)$, and $\phi_r(t)$ are such that

$$y(x,t) = t\left(\frac{e^{-x/\sqrt{\varepsilon}} + e^{-(1-x)/\sqrt{\varepsilon}}}{1 + e^{-1/\sqrt{\varepsilon}}} - \cos^2(\pi x)\right).$$

The surface plot in Fig. 2 displays the numerical solutions of Example 4.2 for $\varepsilon = 10^{-4}$ with $N=128$ and $M=32$. This clearly shows the existence of boundary layers near $x=0$ and $x=1$. We calculate the pointwise errors using the formula

$$G_{i,k}^{\varepsilon,N,M} = |Y_i^k - y(x_i^k, t_k)|.$$

After that the errors $G^{\varepsilon,N,M}$ and $G^{N,M}$, and convergence rates $F^{\varepsilon,N,M}$ and $F^{N,M}$ are computed as described earlier. Table 3 displays the numerical results for Example 4.2, where the last two rows represents the parameter-uniform errors and the parameter-uniform rates of convergence. In this table, observe that N and M are increasing with the same ratio. From this table, we can deduce that the rate of convergence is two. Note that in this case the space discretization errors are dominating the global errors.

In summary, we observe that the proposed numerical method is parameter-uniformly convergent of order two in space and order one in time. Further, the assumption $N^{-\gamma} \le C\Delta t$ is not necessary in practice.

Table 3
Errors and convergence rates for Example 4.2.

ε	$N = 32$ $M = 8$	$N = 64$ $M = 16$	$N = 128$ $M = 32$	$N = 256$ $M = 64$	$N = 512$ $M = 128$
10^0	1.5235e−03	3.9133e−04	1.0052e−04	2.5109e−05	6.2779e−06
	1.9610	1.9609	2.0012	1.9998	
10^{-1}	1.3209e−03	3.3450e−04	8.4770e−05	2.1185e−05	5.2967e−06
	1.9814	1.9804	2.0005	1.9999	
10^{-2}	2.5805e−03	6.2775e−04	1.5569e−04	3.8792e−05	9.6878e−06
	2.0394	2.0115	2.0048	2.0015	
10^{-3}	7.8877e−03	2.0397e−03	4.7116e−04	1.1462e−04	2.8424e−05
	1.9513	2.1140	2.0394	2.0117	
10^{-4}	1.3994e−02	3.2189e−03	7.6427e−04	1.8904e−04	4.8325e−05
	2.1202	2.0744	2.0154	1.9678	
10^{-5}	1.9291e−02	4.0366e−03	9.7065e−04	2.3620e−04	5.8728e−05
	2.2567	2.0561	2.0389	2.0079	
10^{-6}	2.3577e−02	4.5430e−03	1.0548e−03	2.5887e−04	6.3981e−05
	2.3757	2.1066	2.0267	2.0165	
10^{-7}	2.7531e−02	4.8054e−03	1.1034e−03	2.6761e−04	6.6108e−05
	2.5183	2.1227	2.0438	2.0172	
10^{-8}	2.8902e−02	5.2693e−03	1.1260e−03	2.7197e−04	6.6985e−05
	2.4555	2.2264	2.0497	2.0215	
$G^{N,M}$	2.8902e−02	5.2693e−03	1.1260e−03	2.7197e−04	6.6985e−05
$F^{N,M}$	2.4555	2.2264	2.0497	2.0215	

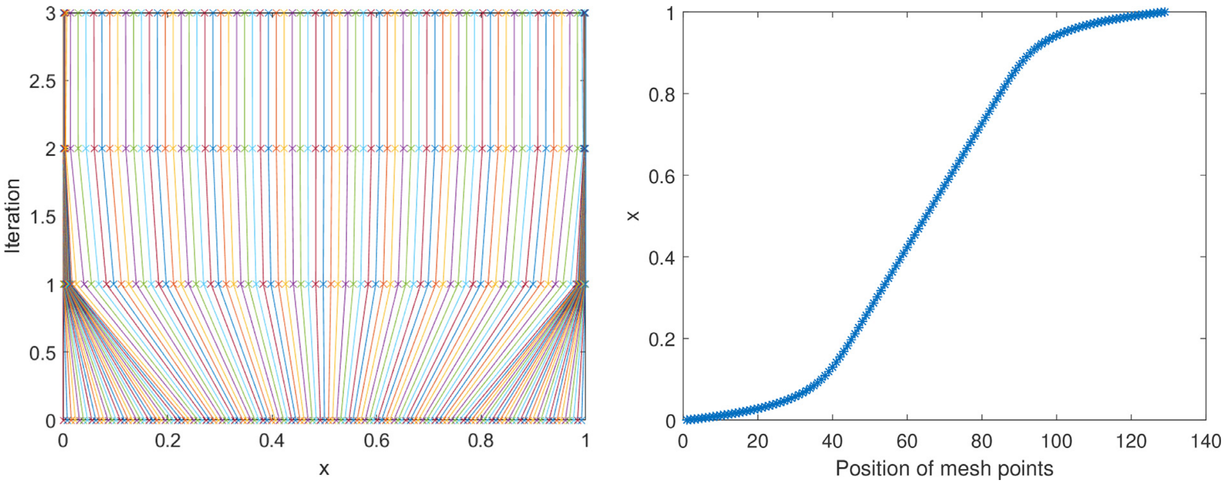

Fig. 3. Mesh trajectory and position of space mesh points taking $N = 128$, $M = 32$, and $\varepsilon = 10^{-5}$ for Example 4.1.

At the first time level t_1, we have shown the adaptive movement of spatial mesh points for Examples 4.1 and 4.2 in Figs. 3 and 4, respectively. These figures display the condensation of mesh points towards the boundary layers in few iterations and finally the adaptation of solution behavior by itself. In Fig. 5, we have plotted the log-log graphs of the maximum pointwise errors versus the number of spatial mesh points N for both test examples. The slopes of these plots also validate the theoretically obtained convergence result in space.

5. Conclusions

A parameter-uniform adaptive mesh method is introduced for a class of singularly perturbed parabolic reaction-diffusion problems with RBCs. The adaptive mesh is generated using the equidistribution principle and the main advantage is that it does not require a priori information about the location of the boundary layers. The method is proved to be parameter-uniformly convergent of order two in space and order one in time. The theoretical error bound is supported by the numerical results.

Acknowledgements

This research was supported by the Science and Engineering Research Board (SERB) under the Project no. ECR/2017/000564. The second author gratefully acknowledge the support of University Grant Commission, India, for re-

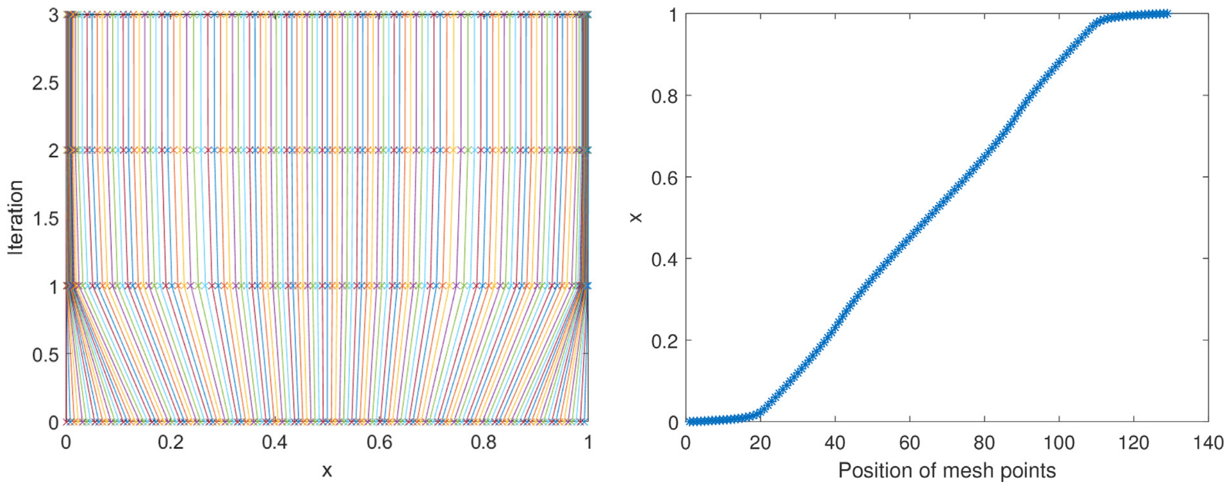

Fig. 4. Mesh trajectory and position of space mesh points taking $N = 128$, $M = 32$, and $\varepsilon = 10^{-5}$ for Example 4.2.

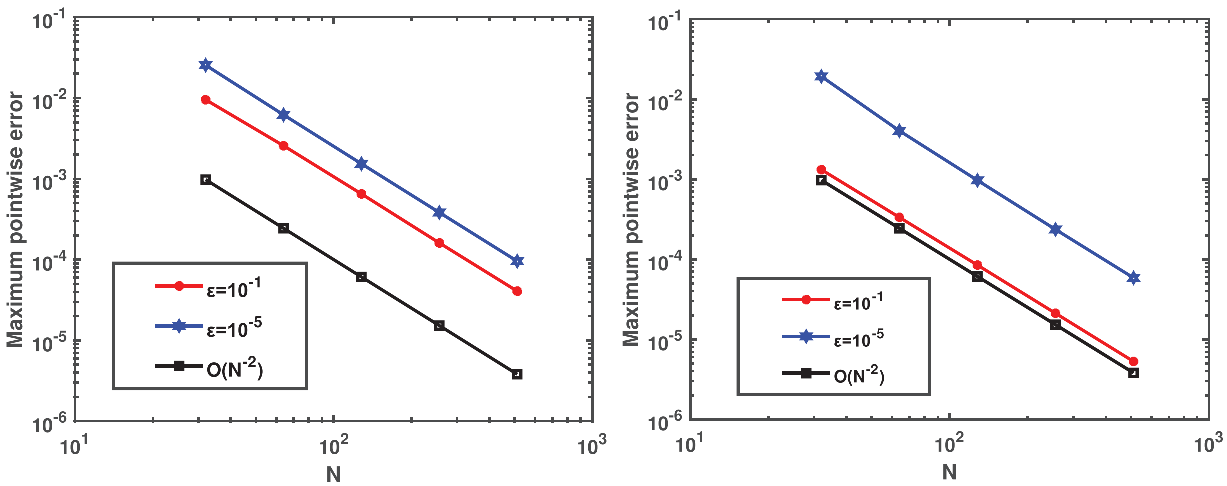

Fig. 5. Log-log plots of the maximum pointwise error for Examples 4.1 (left) and 4.2 (right).

search fellowship with reference no. 20/12/2015(ii)EU-V. The authors gratefully acknowledge the valuable comments and suggestions from the anonymous referees.

Appendix A. A stationary problem

The stationary version of problem (1.1) is an important ingredient needed to study the time dependent problem (1.1). So, this appendix is devoted to the parameter-uniform convergence analysis of a finite difference scheme (similar to (2.1)) on equidistributed meshes for the following stationary problem

$$\begin{cases} \mathcal{L}_\varepsilon y := -\varepsilon \frac{d^2y}{dx^2} + a(x)y = f(x), \quad x \in (0,1), \\ \mathcal{D}_{l,x} y(0) := y(0) - \sqrt{\varepsilon}\frac{dy}{dx}(0) = \phi_l, \\ \mathcal{D}_{r,x} y(1) := y(1) + \sqrt{\varepsilon}\frac{dy}{dx}(1) = \phi_r. \end{cases} \tag{A.1}$$

We assume that the functions $a(x)$ and $f(x)$ are sufficiently smooth and that $0 < \alpha \le a(x)$, $x \in [0, 1]$. This problem has been previously studied in Das and Natesan [13], where y is decomposed as $y = v + w$, and the following bounds were obtained

$$\left|\frac{d^p v(x)}{dx^p}\right| \le C(1 + \varepsilon^{1-p/2}), \tag{A.2}$$

$$\left|\frac{d^p w(x)}{dx^p}\right| \le C\varepsilon^{-\frac{p}{2}}\left(e^{-x\sqrt{\frac{\alpha}{\varepsilon}}} + e^{-(1-x)\sqrt{\frac{\alpha}{\varepsilon}}}\right), \ 0 \le p \le 4, x \in [0,1]. \tag{A.3}$$

A coupled system of two stationary problems with RBCs is studied in Das et al. [19]. In [13,19], for boundary conditions a scheme based on cubic splines is used and for interior points differential equation is discretized using the classical central difference scheme. But, here we discretize problem (A.1) using a scheme similar to (2.1). The discretization is as follows

$$\begin{cases} \left[L_\varepsilon^N Y\right]_i := -\varepsilon\delta_x^2 Y_i + a_i Y_i = f_i, \quad i = 1,\dots,N-1, \\ \left[D_{l,x}^N Y\right]_0 := Y_0 - \sqrt{\varepsilon}D_x^+ Y_0 + \frac{h_1}{2\sqrt{\varepsilon}} a_0 Y_0 = \phi_l + \frac{h_1}{2\sqrt{\varepsilon}} f_0, \\ \left[D_{r,x}^N Y\right]_N := Y_N + \sqrt{\varepsilon}D_x^- Y_N + \frac{h_N}{2\sqrt{\varepsilon}} a_N Y_N = \phi_r + \frac{h_N}{2\sqrt{\varepsilon}} f_N, \end{cases} \tag{A.4}$$

where the difference operators D_x^+, D_x^- and δ_x^2 defined analogously as for the discretization (2.1), and the mesh $\{x_i\}_{i=0}^N$ is the following equidistributed mesh with step sizes $h_i = x_i - x_{i-1}$, where

$$\frac{i}{N}\left(\frac{\aleph}{\mathbf{A}} + 1\right) = \frac{\aleph}{\mathbf{A}} x_i + \lambda_1\left(1 - e^{-\frac{x_i}{2}\sqrt{\frac{\alpha}{\varepsilon}}}\right), \quad x_i \le 1/2 \tag{A.5}$$

and

$$\left(1 - \frac{i}{N}\right)\left(\frac{\aleph}{\mathbf{A}} + 1\right) = \frac{\aleph}{\mathbf{A}}(1 - x_i) + \lambda_2\left(1 - e^{-\frac{(1-x_i)}{2}\sqrt{\frac{\alpha}{\varepsilon}}}\right), \quad x_i > 1/2, \tag{A.6}$$

which is obtained using the monitor function $\mathcal{M} = \aleph + |\frac{d^2 w}{dx^2}|^{1/2}$ (see Section 2 for details). The discretization (A.4) satisfies the following discrete maximum principle which can be proved using standard arguments [8].

Lemma 3. *(Discrete maximum principle) Consider a mesh function U such that $[L_\varepsilon^N U]_i \ge 0$ for $i = 1,\dots,N-1$, and $[D_{l,x}^N U]_0 \ge 0$, $[D_{r,x}^N U]_N \ge 0$. Then $U_i \ge 0$ for $i = 0,\dots,N$.*

Theorem A.1. *Let y and Y be the solutions of (A.1) and (A.4), respectively. Then, for $i = 0,\dots,N$, we have*

$$|y(x_i) - Y_i| \le CN^{-2}.$$

Proof. At the left boundary, we proceed as follows

$$\begin{aligned} [D_{l,x}^N (y - Y)]_0 &= [D_{l,x}^N y]_0 - \left(\phi_l + \frac{h_1}{2\sqrt{\varepsilon}} f_0\right) \\ &= \left[y(x_0) - \sqrt{\varepsilon}D_x^+ y(x_0) + \frac{h_1}{2\sqrt{\varepsilon}} a_0 y(x_0)\right] - \left[y(x_0) - \sqrt{\varepsilon}\frac{dy}{dx}(x_0) + \frac{h_1}{2\sqrt{\varepsilon}} f_0\right] \\ &= \sqrt{\varepsilon}\left(\frac{dy}{dx}(x_0) - D_x^+ y(x_0)\right) + \frac{h_1}{2\sqrt{\varepsilon}}\left(a_0 y(x_0) - f_0\right) \\ &= \sqrt{\varepsilon}\left(\frac{dy}{dx}(x_0) - D_x^+ y(x_0)\right) + \frac{h_1\sqrt{\varepsilon}}{2}\frac{d^2 y}{dx^2}(x_0) \\ &= -\frac{h_1^2\sqrt{\varepsilon}}{6}\frac{d^3 y}{dx^3}(\eta) \text{ for some } \eta \in (x_0, x_1). \end{aligned}$$

Now using the solution decomposition we have

$$|[D_{l,x}^N (y - Y)]_0| = \frac{h_1^2\sqrt{\varepsilon}}{6}\left|\frac{d^3 y}{dx^3}(\eta)\right| \le \frac{h_1^2\sqrt{\varepsilon}}{6}\left|\frac{d^3 v}{dx^3}(\eta)\right| + \frac{h_1^2\sqrt{\varepsilon}}{6}\left|\frac{d^3 w}{dx^3}(\eta)\right|.$$

Using the derivative bounds of v from (A.2) and Lemma 2, we get

$$h_1^2\sqrt{\varepsilon}\frac{d^3 v}{dx^3}(\eta) \le CN^{-2}.$$

For the layer component, we use the derivative bounds from (A.3) and proceed as follows

$$\begin{aligned} h_1^2\sqrt{\varepsilon}\tfrac{d^3 w}{dx^3}(\eta) &\le C\varepsilon^{-1} h_1^2 e^{-x_0\sqrt{\frac{\alpha}{\varepsilon}}} \\ &\le C\varepsilon^{-1}\left(\int_{x_0}^{x_1} e^{-\frac{z}{2}\sqrt{\frac{\alpha}{\varepsilon}}} dz\right)^2 \le C\varepsilon^{-1}\left(\sqrt{\varepsilon}\int_{x_0}^{x_1}\mathcal{M}(y(z), z) dz\right)^2 \\ &\le C\mathbf{A}^2 N^{-2} \le CN^{-2}. \end{aligned}$$

Hence

$$|[D_{l,x}^N (y - Y)]_0| \le CN^{-2}. \tag{A.7}$$

Similarly

$$|[D_{r,x}^N (y - Y)]_N| \le CN^{-2}. \tag{A.8}$$

We can use the arguments in Beckett and Mackenzie [17] to show that

$$|[L_\varepsilon^N (y - Y)]_i| \le CN^{-2} \quad \text{for } i = 1,\dots,N-1. \tag{A.9}$$

Thus, we consider the barrier function $\Psi_i^{\pm} = CN^{-2} \pm (y(x_i) - Y_i)$ and use the discrete maximum principle (Lemma 3) to get the desired result. □

References

[1] H.-G. Roos, M. Stynes, L. Tobiska, Robust numerical methods for singularly perturbed differential equations, Springer Series in Computational Mathematics, second ed., Springer-Verlag, Berlin, 2008.
[2] S. Kumar, M. Kumar, Parameter-robust numerical method for a system of singularly perturbed initial value problems, Numer. Algorithms 59 (2) (2012) 185–195.
[3] M.K. Kadalbajoo, V. Gupta, A brief survey on numerical methods for solving singularly perturbed problems, Appl. Math. Comput. 217 (8) (2010) 3641–3716.
[4] S. Kumar, Layer-adapted methods for quasilinear singularly perturbed delay differential problems, Appl. Math. Comput. 233 (2014) 214–221.
[5] S. Kumar, M. Kumar, Analysis of some numerical methods on layer adapted meshes for singularly perturbed quasilinear systems, Numer. Algorithms 71 (1) (2016) 139–150.
[6] M. Chandru, P. Das, H. Ramos, Numerical treatment of two-parameter singularly perturbed parabolic convection diffusion problems with non-smooth data, Math. Methods Appl. Sci. 41 (14) (2018) 5359–5387.
[7] P. Hemker, G. Shishkin, L. Shishkina, The numerical solution of a neumann problem for parabolic singularly perturbed equations with high-order time accuracy, in: Recent Advances in Numerical Methods and Applications II, World Scientific, 1999, pp. 27–39.
[8] P.A. Selvi, N. Ramanujam, A parameter uniform difference scheme for singularly perturbed parabolic delay differential equation with Robin type boundary condition, Appl. Math. Comput. 296 (2017) 101–115.
[9] S.C.S. Rao, S. Kumar, Second order global uniformly convergent numerical method for a coupled system of singularly perturbed initial value problems, Appl. Math. Comput. 219 (8) (2012) 3740–3753.
[10] G. Shishkin, A difference scheme for a singularly perturbed equation of parabolic type with discontinuous boundary conditions, USSR Comput. Math. Math. Phys. 28 (6) (1988) 32–41.
[11] N.S. Bakhvalov, On the optimization of the methods for solving boundary value problems in the presence of a boundary layer, Zhurnal Vychislitel'noi Mat. Matematicheskoi Fiziki 9 (4) (1969) 841–859.
[12] W. Huang, R.D. Russell, Adaptive Moving Mesh Methods, 174, Springer Science & Business Media, 2010.
[13] P. Das, S. Natesan, Higher-order parameter uniform convergent schemes for Robin type reaction-diffusion problems using adaptively generated grid, Int. J. Comput. Methods 9 (04) (2012) 1250052.
[14] Y. Qiu, D. Sloan, Analysis of difference approximations to a singularly perturbed two-point boundary value problem on an adaptively generated grid, J. Comput. Appl. Math. 101 (1–2) (1999) 1–25.
[15] J. Mackenzie, Uniform convergence analysis of an upwind finite-difference approximation of a convection-diffusion boundary value problem on an adaptive grid, IMA J. Numer. Anal. 19 (2) (1999) 233–249.
[16] S. Gowrisankar, S. Natesan, The parameter uniform numerical method for singularly perturbed parabolic reaction-diffusion problems on equidistributed grids, Appl. Math. Lett. 26 (11) (2013) 1053–1060.
[17] G. Beckett, J.A. Mackenzie, On a uniformly accurate finite difference approximation of a singularly perturbed reaction–diffusion problem using grid equidistribution, J. Comput. Appl. Math. 131 (1–2) (2001) 381–405.
[18] N. Kopteva, N. Madden, M. Stynes, Grid equidistribution for reaction–diffusion problems in one dimension, Numer. Algorithms 40 (3) (2005) 305–322.
[19] P. Das, S. Rana, J. Vigo-Aguiar, Higher order accurate approximations on equidistributed meshes for boundary layer originated mixed type reaction diffusion systems with multiple scale nature, Appl. Numer. Math. 148 (2020) 79–97.
[20] L.-B. Liu, G. Long, Z. Cen, A robust adaptive grid method for a nonlinear singularly perturbed differential equation with integral boundary condition, Numer. Algorithms 83 (2) (2020) 719–739.
[21] P. Das, V. Mehrmann, Numerical solution of singularly perturbed convection-diffusion-reaction problems with two small parameters, BIT Numer. Math. 56 (1) (2016) 51–76.
[22] P. Das, Comparison of a priori and a posteriori meshes for singularly perturbed nonlinear parameterized problems, J. Comput. Appl. Math. 290 (2015) 16–25.
[23] P. Das, An a posteriori based convergence analysis for a nonlinear singularly perturbed system of delay differential equations on an adaptive mesh, Numer. Algorithms 81 (2019) 465–487.
[24] J. Singh, S. Kumar, M. Kumar, A domain decomposition method for solving singularly perturbed parabolic reaction-diffusion problems with time delay, Numer. Methods Partial Differ. Equ. 34 (5) (2018) 1849–1866.
[25] T. Linß, N. Madden, Parameter uniform approximations for time-dependent reaction-diffusion problems, Numer. Methods Partial Differ. Equ. 23 (6) (2007) 1290–1300.
[26] J.J.H. Miller, E. O'Riordan, G.I. Shishkin, L.P. Shishkina, Fitted mesh methods for problems with parabolic boundary layers, in: Mathematical Proceedings-Royal Irish Academy, 98, Royal Irish Academy, 1998, pp. 173–190.
[27] C. Clavero, J.L. Gracia, High order methods for elliptic and time dependent reaction–diffusion singularly perturbed problems, Appl. Math. Comput. 168 (2) (2005) 1109–1127.
[28] S. Kumar, S.C.S. Rao, A robust overlapping Schwarz domain decomposition algorithm for time-dependent singularly perturbed reaction–diffusion problems, J. Comput. Appl. Math. 261 (2014) 127–138.
[29] S.C.S. Rao, S. Kumar, J. Singh, A discrete Schwarz waveform relaxation method of higher order for singularly perturbed parabolic reaction-diffusion problems, J. Math. Chem. 58 (2020) 574–594.
[30] S. Kumar, M. Kumar, High order parameter-uniform discretization for singularly perturbed parabolic partial differential equations with time delay, Comput. Math. Appl. 68 (10) (2014) 1355–1367.
[31] M. Kumar, S.C.S. Rao, High order parameter-robust numerical method for time dependent singularly perturbed reaction-diffusion problems, Computing 90 (2010) 15–38.
[32] P. Hemker, G. Shishkin, L. Shishkina, High-order time-accurate schemes for singularly perturbed parabolic convection-diffusion problems with Robin boundary conditions, Comput. Methods Appl. Math. 2 (2002) 3–25.
[33] R. Ishwariya, J.J.H. Miller, S. Valarmathi, A parameter uniform essentially first order convergent numerical method for a parabolic singularly perturbed differential equation of reaction-diffusion type with initial and Robin boundary conditions, 2019, arXiv:1906.01598.
[34] P. Das, J. Vigo-Aguiar, Parameter uniform optimal order numerical approximation of a class of singularly perturbed system of reaction diffusion problems involving a small perturbation parameter, J. Comput. Appl. Math. 354 (2019) 533–544.
[35] R.B. Kellogg, A. Tsan, Analysis of some difference approximations for a singular perturbation problem without turning points, Math. Comput. 32 (144) (1978) 1025–1039.
[36] C. Clavero, J.L. Gracia, M. Stynes, A simpler analysis of a hybrid numerical method for time-dependent convection–diffusion problems, J. Comput. Appl. Math. 235 (17) (2011) 5240–5248.